

# Fluid-Structure Interaction Heat Transfer of Piston with Consideration of Oil Oscillating Cooling and In-Cylinder Local Heat Transfer

Xiaori Liu<sup>a</sup>, Dongkang Cheng<sup>a</sup>, Jingjing Zhou<sup>b</sup>, Qingping Zheng<sup>\*,a</sup>, Xue Mi<sup>a</sup>  
 Su Li<sup>a</sup>, Guoxiang Li<sup>c</sup>

<sup>a</sup>School of Energy and Environmental Engineering, Hebei University of Technology, Tianjin 300401, China

<sup>b</sup>School of Automotive Engineering, Tianjin Vocational Institute, Tianjin 300410, China

<sup>c</sup>School of Energy and Power Engineering, Shandong University, Jinan 250061, China  
 qpzh163@163.com

Taking the piston of heavy commercial vehicle as an example, in-cylinder local heat transfer boundary condition is obtained through the calculation of intake, spray, combustion and exhaust process; the heat transfer boundaries of the inner oil gallery and the bottom of the piston are obtained by the transient piston injection cooling calculation; the numerical simulation of temperature field of piston is realized by the coupling of gas side, lubrication oil side and structure with consideration of the temperature's influence on the thermal conductivity of the piston. Furthermore, the thermal deformation of the piston is analysed. Results show that the calculated values are in agreement with the experimental temperature values of the piston measuring points; The highest temperature appears at the junction of the bowl and the top surface of the piston at the exhaust valve side; The heat transfer coefficient and gas temperature at the junction of the bowl and the top surface of the piston are in high value, the in-cylinder local heat transfer is significant; In the straight inlet pipe of the inner oil gallery, the temperature of the lube oil is the lowest while heat transfer coefficient is the highest, so the cooling effect is the most obvious; The radial expansion deformation is large at the top and bottom of the piston skirt while small at the middle.

## 1. Introduction

Piston-cylinder liner friction pair is one of the most important mechanical loss sources in internal combustion engine (Wu et al., 2012). With increasing power density, the heat load of internal combustion engine becomes more and more serious. The influence of piston heat load on frictional power loss is more prominent (Johansson et al., 2011) and the heat load is also has effect on the blow-by of the piston ring (Liu et al., 2015). During intake, spray, combustion and exhaust process, the piston top is heated by high temperature gas in cylinder and influenced by turbulence fluctuation, spray breakup and wall impingement, ignition and combustion, and so on (Guzmán et al., 2015). To reduce the heat load, piston is often cooled with lube oil injected into its inner cooling gallery. During the piston injected cooling, piston is influenced by multiphase flow oscillation heat transfer because of its high reciprocating motion. So it is necessary to consider the combined effect of in-cylinder local heat transfer and lube oil oscillating cooling in the calculation of piston temperature field.

Empirical formula or experience values by regions are often used for the heat transfer boundary of gas side of piston top surface. The Woschni formula has been used by many researchers for different kinds of engines, such as marine diesel engine (Lu et al., 2013), commercial vehicle diesel engine (Zu et al., 2014), diesel-natural gas dual fuel engine (Ning et al., 2014) and high-speed diesel engine (Li et al., 2015). Ba et al. (2014) improved the heat transfer boundary of piston top surface with consideration of the local cooling effect of the intake process. The heat transfer boundaries of piston inner cooling gallery and piston bottom are used empirical formula mostly. Yuan et al. (2008) used empirical values for piston inner cooling gallery and piston bottom. The area-average Nusselt number correlations for piston inner cooling gallery were derived by Easter et al. (2014)

based on laboratory tests. Lu et al. (2017) got the heat transfer coefficient of the cooling cavity of piston with the empirical formulas by Bush and French, and piston bottom with empirical value. Wu et al. (2015) simulated the piston temperature field with the time integral average boundary of transient results from CFD calculation in annular inner gallery.

Taking the piston of heavy commercial vehicle as an example, the local heat transfer boundary of piston top is obtained through the calculation of intake, spray, combustion and exhaust process; The heat transfer boundaries of piston inner cooling oil chambers and piston bottom are obtained by transient piston injection cooling calculation; The numerical simulation of temperature field of piston is realized by the coupling of gas side, lubrication oil side and structure with consideration of the temperature's influence on the thermal conductivity of the piston; At the same time, the thermal deformation of the piston is further obtained in order to provide reference for the low friction design of the piston-cylinder liner conjunction.

## 2. Calculation flow of fluid-structure interaction heat transfer

Average heat transfer coefficient and effective average temperature are adopted on the gas side and the oscillating lube oil side.

Average heat transfer coefficient:

$$h_m = \frac{1}{4\pi} \int_0^{4\pi} h_{trans} d\Phi \quad (1)$$

Effective average temperature:

$$T_{eff} = \frac{1}{h_m} \int_0^{4\pi} h_{trans} T_{trans} d\Phi \quad (2)$$

Where  $h_{trans}$  is transient convective heat transfer coefficient,  $T_{trans}$  is transient fluid temperature,  $\Phi$  is crank angle. Taking a heavy duty commercial vehicle diesel engine as the research object,  $1,900 \text{ r}\cdot\text{min}^{-1}$  is chosen as the simulation case. (i) Boundary conditions for in-cylinder 3D combustion calculation are calculated from one-dimensional engine work process. The transient processes of intake, spray, combustion, power and exhaust have been calculated with 3D model in order to get the average heat transfer coefficient and effective average gas temperature of gas side at the top surface of the piston. (ii) The transient injected cooling of the piston is calculated by VOF method to get the heat transfer boundary conditions of the inner cooling oil gallery and the bottom surface of the piston. (iii) The heat transfer boundary data of piston top surface, inner cooling oil gallery and piston bottom surface are mapped to the finite element mesh grids to calculate the piston temperature field and the accuracy of the calculation results are verified by the measuring temperature data. (iv) Thermal deformation of piston skirt is obtained based on the calculation results of temperature field. In addition, the heat transfer boundaries of piston ring groove, piston ring bank and piston skirt are set according to experience values.

Two cases of transient translational boundaries for the piston are shown in Figure 1. The data mapping between fluid and structure is programmed in Python.

(i) Inner cooling gallery and bottom surface: Fluent software is used to calculate oil oscillating cooling. The position of FEA coupling surface mesh should be synchronized with the piston displacement. After the completion of the data mapping, the heat transfer coefficient and temperature should be numerical integration in the range of  $720^\circ$  crank angle and then done time average according to Eqs(1) and (2).

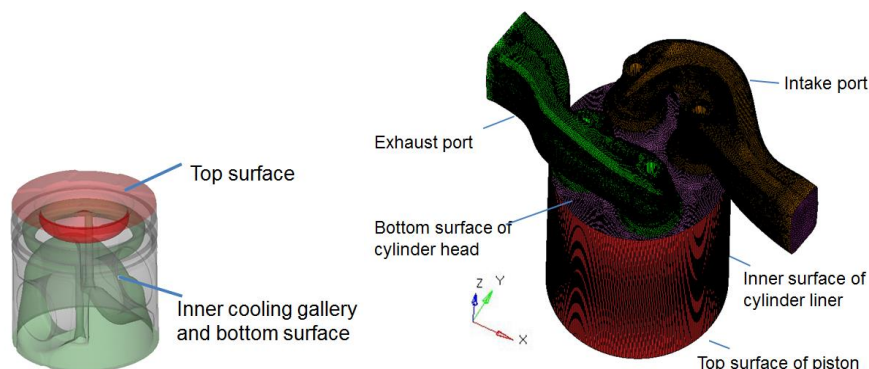


Figure 1: Transient translational boundaries      Figure 2: Surface mesh of in-cylinder CFD calculation at BDC

(ii) Top surface: The in-cylinder CFD is calculated with the Converge software. For the transient motion boundary, the calculated results of Converge software refer to the transient coordinates as well as the original

coordinates at the position of bottom dead centre (BDC). The position of FEA coupling surface mesh could be always maintained at BDC. According to Eq(1) and Eq(2), average heat transfer coefficient and effective average temperature are calculated. Finally, the data mapping is completed.

### 3. Heat transfer of the piston

#### 3.1 Heat transfer boundary of gas side

The surface mesh at BDC is provided, and the 3D grids are automatically generated during simulation. Figure 2 shows the surface mesh of CFD in cylinder at BDC.

The models used for in-cylinder CFD calculation are as follows: RNG k- $\epsilon$  turbulence model, Redlich-Kwong equation of state, KH-RT spray breakup length model, Naber-Reitz wall impingement model, Shell ignition model and the Characteristic Time Combustion (CTC) model, etc. (Liu et al., 2014)

The average heat transfer coefficient and effective average temperature of the gas side at the top surface of the piston are shown in Figure 3. The heat transfer coefficient and gas temperature at the junction of the bowl and the top surface of the piston are in high value, the in-cylinder local heat transfer is significant.

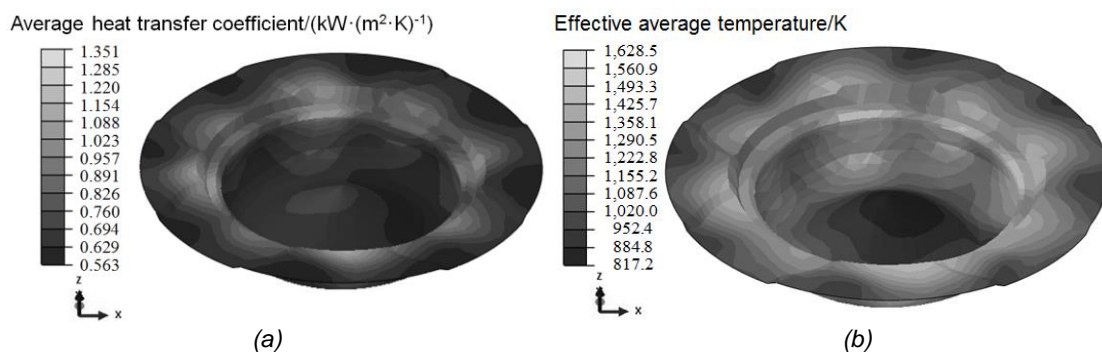


Figure 3: Gas side boundary: (a) Average heat transfer coefficient, (b) Effective average temperature

#### 3.2 Heat transfer boundaries of inner cooling oil gallery and bottom surface

The lube oil is injected into the piston oil gallery from an injector fixed on the engine body. As the piston reciprocating within the cylinder liner, the oil oscillates in the inner oil gallery and finally flows back into the oil pan. The flow region is walled by an inner oil gallery, a piston bottom surface and a cylinder liner inner surface which are all the translational moving boundaries, inlet and outlet of the cooling oil are both stationary boundaries. The mesh of oil oscillating cooling at BDC is shown in Figure 4.

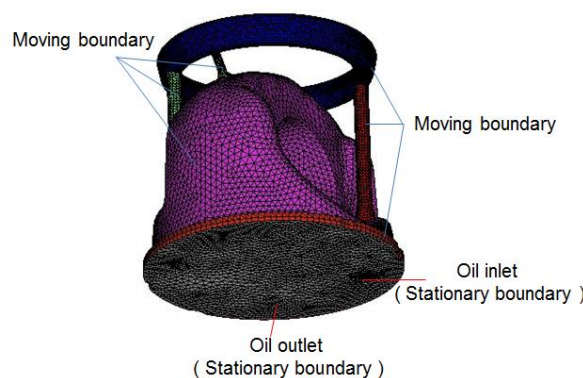


Figure 4: The mesh of oil oscillating cooling at BDC

The boundary conditions are as follows: Inlet flow rate is 7 L/min; Outlet pressure is 0 Pa; Wall temperature is set to 433 K. Initially, the entire fluid region is filled with air; VOF model is used which takes air as the first phase and cooling oil as second phase. The cooling oil volume fraction is 1 at the inlet position.

The calculated average heat transfer coefficient and effective average temperature of the piston inner cooling oil gallery and piston bottom are shown in Figure 5. In the straight inlet pipe of the inner oil gallery, the

temperature of the lube oil is the lowest while heat transfer coefficient is the highest, so the cooling effect is the most obvious.

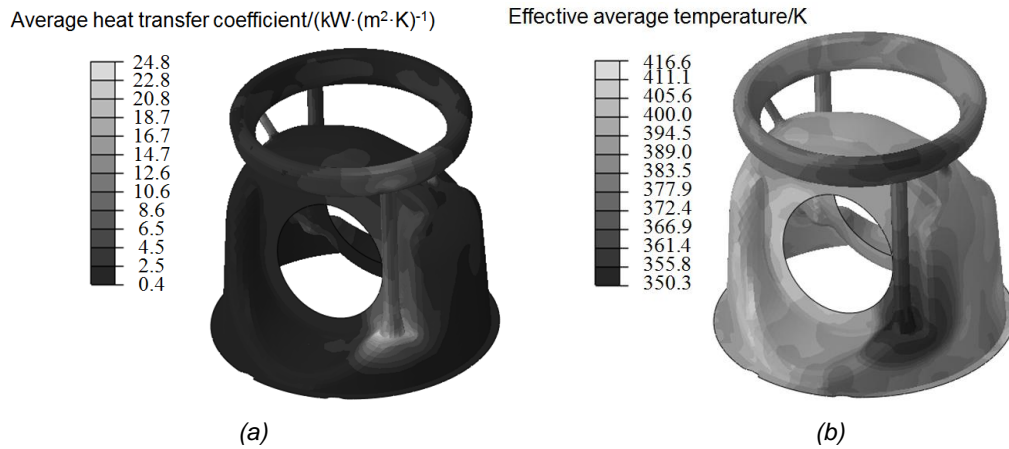


Figure 5: Oil side boundary: (a) Average heat transfer coefficient, (b) Effective mean temperature

**3.3 Heat transfer boundary conditions of the other regions**

The heat transfer coefficient and temperature of the other regions are shown in Table 1.

Table 1: Heat transfer boundary conditions of the other regions

Region	Heat transfer coefficient $W \cdot (m^2 \cdot K)^{-1}$	Temperature K
Bank above 1st piston ring	427	673
Bank between 1st and 2nd piston ring	427	523
Bank between 2nd and 3rd piston ring	197	423
Top surface of 1st ring groove	486	423
Flank of 1st ring groove	265	423
Bottom surface of 1st ring groove	2,570	423
Top surface of 2nd ring groove	634.7	393
Flank of 2nd ring groove	611.6	393
Bottom surface of 2nd ring groove	1,596	393
Top surface of 3rd ring groove	2,000	393
Flank of 3rd ring groove	686	393
Bottom surface of 3rd ring groove	2,000	393
piston skirt	2,728	363

**3.4 Temperature field of the piston**

The mesh of temperature field calculation is shown in Figure 6. Computational coordinate system: The piston pin centre is (0, 0, 0), the positive Z axis is point to the cylinder head, the X axis is along with the axial axis of the pin seat, the positive X axis is from the exhaust valve side to the inlet valve side.

Piston material is aluminium alloy. The influence of temperature on the thermal conductivity of piston is considered in the calculation. Material properties for calculation are shown in Table 2.

Table 2: Material properties of piston

Material name	Temperature K	Thermal conductivity $W \cdot (m \cdot K)^{-1}$	Elastic modulus GPa	Thermal expansion coefficient 1/K	Poisson ratio
Aluminium alloy	293	120.0	70	2.51e-05	0.3
	373	152.0			
	423	158.0			
	473	163.0			
	523	170.0			
	573	175.0			

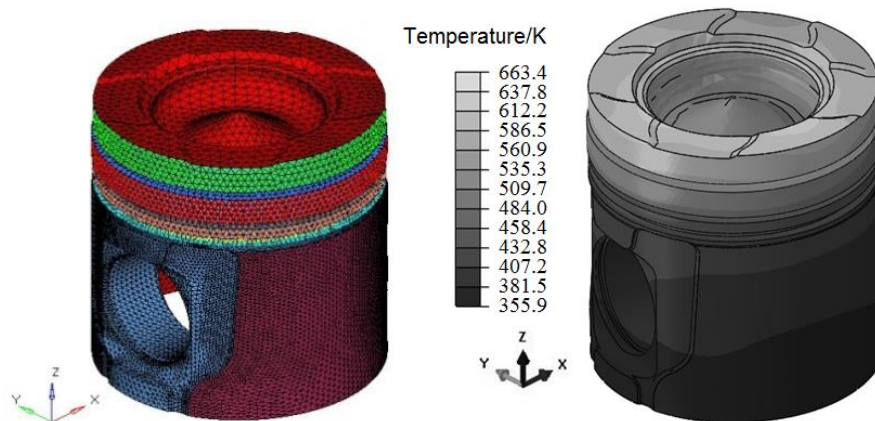


Figure 6: The mesh of temperature field calculation      Figure 7: Calculation results of temperature field

Figure 7 shows the calculation results of piston temperature field. The spatial distribution of temperature field is not symmetrical. The highest temperature (663.4 K) appears at the junction of the bowl and the top surface of the piston at the exhaust valve side. The minimum temperature (355.9 K) appears at the bottom of piston skirt. Figure 8 shows the temperature measuring positions of the piston. The temperatures are measured by 20 hardness plugs. The maximum error is 8.33 % while the average error is 1.73 %. (Figure 9)

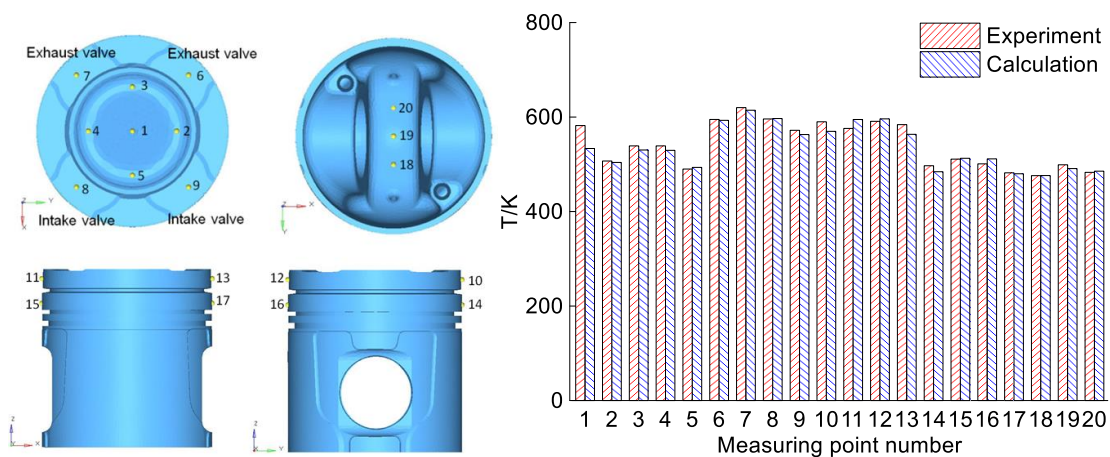


Figure 8: Measuring positions      Figure 9: Comparisons between measured and calculated values

**4. Deformation**

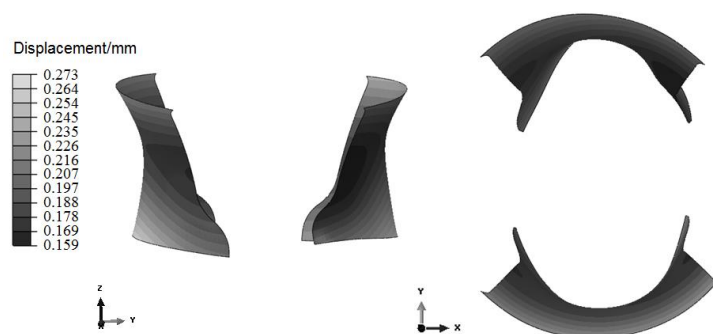


Figure 10: Deformation of piston skirt



Calculation of piston thermal deformation is based on the result of piston temperature field. Figure 10 shows the deformation of the piston skirt, the displayed deformation is increased by 500 times to observe the trend. In the YOZ plane, the radial expansion deformation is large at the top and bottom of the piston skirt while small at the middle. In the XOY plane, larger displacement in the Y direction results in the elliptical deformation shape. The top of the piston skirt is close to the circle while the ellipticity of the bottom is larger.

## 5. Conclusions

Fluid-structure interaction heat transfer of piston is calculated with consideration of lube oil oscillating cooling and in-cylinder local heat transfer. The data mapping between fluid and structure is programmed in Python with the average heat transfer coefficient and effective average temperature. The influence of temperature on the thermal conductivity of piston is considered. The calculated values are in agreement with the experimental temperature values of the piston measuring points. The spatial distributions of heat transfer boundary conditions, temperature field and deformation are not symmetrical.

## Acknowledgments

This work was supported by the National Natural Science Foundation of China (51576116), Student's Platform for Innovation and Entrepreneurship Training Program (201610080061) and Scientific Research Foundation of the Higher Education Institutions of Hebei Province, China (QN2016041).

## References

- Ba L., Liu Y.H., Li A.H., 2014, Improvement of piston top temperature analysis using intake process CFD simulation, *Transactions of CSICE*, 32(6), 548-554.
- Easter J., Jarrett C., Pespisa C., 2014, An area-average correlation for oil-jet cooling of automotive pistons, *Journal of Heat Transfer*, 136(12), 124501, doi: 10.1115/1.4027835.
- Guzmán M.A., Katherine Ardila L., Agudelo J.R., 2015, Combustion characteristics, performance and emissions of a diesel engine fuelled with water/diesel emulsions, *Chemical Engineering Transactions*, 45, 1039-1044
- Johansson S., Nilsson P.H., Ohlsson R., 2011, Experimental friction evaluation of cylinder liner/piston ring contact, *Wear*, 271, 625-633.
- Li K.Y., Xiao B., Zhang C.W., 2015, Effects of intake air temperature and thermal deformation in a diesel- natural gas dual fuel engine, *Chinese Internal Combustion Engine Engineering*, 36(10), 115-121.
- Liu X.R., Li G.X., Hu Y.P., Bai S.Z., Deng K.Y., 2014, An in-cylinder transient heat transfer model for temperature field simulation of diesel engine structure, *Journal of Shanghai Jiao Tong University*, 48(9), 1286-1290.
- Liu N., Zheng Z.C., Li G.X., 2015, Analysis of the blow-by in piston ring pack of the diesel engine, *Chemical Engineering Transactions*, 46, 1045-1050.
- Lu X.Q., Li Q., Zhang W.P., Guo Y.B., He T., 2013, Thermal analysis on piston of marine diesel engine, *Applied Thermal Engineering*, 50, 168-176.
- Lu Y.H., Zhang X., Xiang P.L., Dong D.W., 2017, Analysis of thermal temperature fields and thermal stress under steady temperature field of diesel engine piston, *Applied Thermal Engineering*, 113, 168-176.
- Ning H.Q., Sun P., Mei D.Q., Xiao S.M., Hu P., 2014, Temperature experimental and thermo-mechanical coupled simulation of high-speed diesel engine piston, *Chinese Internal Combustion Engine Engineering*, 35(1), 105-109.
- Wu B., Ning L.P., Meng X.H., Li J., Xie Y.B., 2012, Tribological simulation and design of piston skirt – liner system to reduce friction of automotive engines, *Tribology*, 32(6), 577-583.
- Wu Q.W., Zhang J.C., Hu Y.P., Xie Z.M., Hu D.Y., Hu Y.P., 2015, Numerical simulation and temperature field analysis of piston oscillating cooling, *Vehicle Engine*, 219(8), 54-59.
- Yuan Y.P., Wang Y., Zhang W.Z., Liu C., Zhao W.M., 2008, Study on the effect upon the piston temperature field through changing the position of the cooling gallery, *Transactions of Beijing Institute of Technology*, 28(7), 585-588.
- Zu B.F., Fang Q., Liu J., Hao C.L., Zhang J.H., 2014, Numerical analysis of piston strength and deformation based on thermo-mechanical coupling for China-V diesel engine, *Chinese Internal Combustion Engine Engineering*, 35(1), 99-104.